fluids

MDPI

Article

Bulbous Pier: An Alternative to Bridge Pier Extensions as a Countermeasure against Bridge Deck Splashing

Moses Karakouzian [1], Amilcar Chavez [1], Donald Hayes [2] and Mohammad Nazari-Sharabian [1,*]

[1] Department of Civil and Environmental Engineering and Construction, University of Nevada Las Vegas, Las Vegas, NV 89154, USA
[2] U.S. Army Engineer Research and Development Center, Vicksburg, MS 39180, USA
* Correspondence: nazarish@unlv.nevada.edu; Tel.: +1-702-205-9336

Received: 27 June 2019; Accepted: 22 July 2019; Published: 24 July 2019

check for updates

Abstract: Bridge deck splashing causes deterioration to a bridge's structure and renders the bridge unsafe for motorists and pedestrians. The traditional countermeasure for bridge deck splashing has been pier extension. Pier extensions move the pier wave and the associated splash away from the bridge deck, but retrofitting existing bridges with pier extensions is costly. This research evaluates the use of a bulbous added to the pier as an alternative to pier extension. A bulb placed on the upstream side of a bridge pier affects the splashing. The energy in the passing water is redirected from the impact by streamlining the flow. This study proposes a mathematical model for bulbous pier design, based on a model used for a mono-hull ship. Under the mono-hull model, the bulb length extends, reaching the region where viscous resistance is dominant. Unlike wave-making resistance, which is achieved through modeling, the proposed model does not require modeling to calculate pier wave reduction.

Keywords: bridge deck splashing; flooding; water spraying problem

1. Introduction

The interaction of supercritical water flow with a pier nose creates a pier wave, which might cause the flowing water to be projected onto the bridge deck. This phenomenon is called bridge deck splashing, and can endanger motorists and pedestrians on the bridge. A solution to this problem is the structural modification of the pier by extending the pier in front of the bridge structure; however, this method is costly. Stonestreet et al. (1994) provided an overview of the extensive physical model studies of the Los Angeles and Rio Hondo rivers [1]. The authors focused on innovative designs that significantly increased the capacity of existing bridges subject to discharges greater than the design discharge. The idea was to extend bridge piers upstream, thereby causing the flow to pass through critical as it accelerates within the pier constriction. Figure 1 illustrates the general profile of the water-surface response to extension of the bridge piers. Illustrations of the effectiveness of these pier extensions are provided in the pictures in Figure 2. The pictures from Hite et al. (1993) are photographs of the 1:50-scale model of the Rio Hondo River [2]. Clearly, the pier extensions eliminated the runup and splash on the bridge deck.

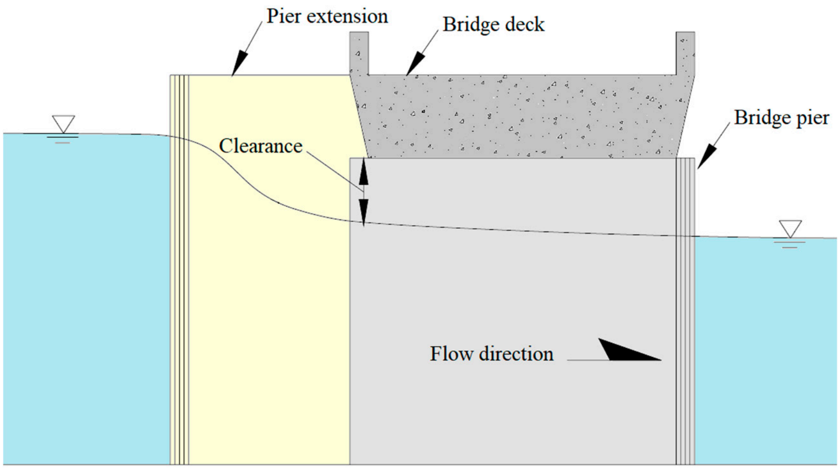

Figure 1. Bridge with pier extension.

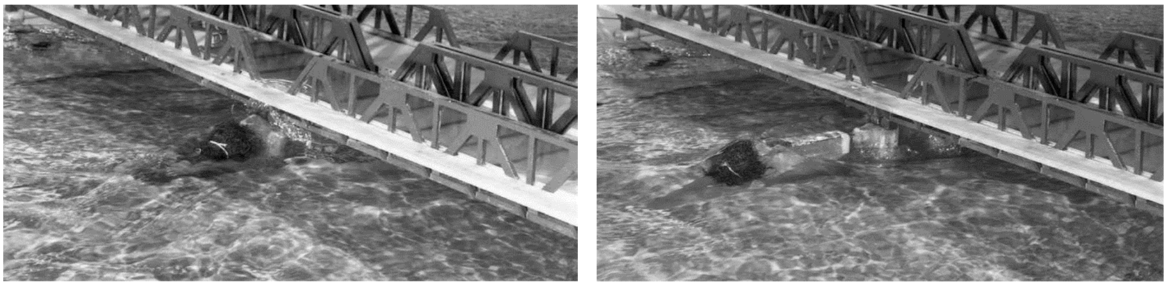

(**a**) (**b**)

Figure 2. (**a**) Flow conditions in 1:50-scale model of the Rio Hondo River, debris on bridge pier, (**b**) Flow conditions in 1:50-scale model of the Rio Hondo River, debris on extended bridge pier [3].

In ships, a bulbous bow is used to mitigate ship deck splashing and reduce propulsion power. A bulbous bow is a flow-modifying feature on a ship's bow, which is considered a countermeasure against ship deck splashing [4]. It creates a wave system that interferes with the ship's natural wave system (Figure 3), which leads to a near-zero wave at the hull-bulb intersection. The water waves created by a moving ship are similar to the water movement around a partially submerged bridge pier. Therefore, the concept of a bulbous bow can reduce the energy available for a pier wave, and as a result, can work as a countermeasure against bridge deck splashing.

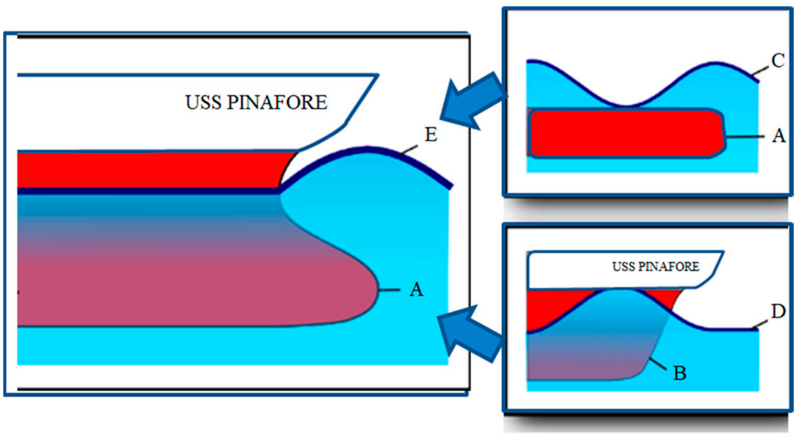

Figure 3. Bulb wave interference principle (**A**) bulb; (**B**) bow; (**C**) bulb wave; (**D**) bow wave; (**E**) combined wave = bow wave − bulb wave.

The study of bulbous bows for high-speed ships has been documented for ship speeds up to 55 knots (92.83 ft./sec.). In the following, the literature review focuses on studies that investigated the effect of bulbous bows in ships with speeds similar to the water velocity in open channels under supercritical conditions. In 1978, Kracht studied the effect of a bulb in relation to ship movement, and concluded that the power required to move a ship is directly related to the total hull resistance [5]. He also showed that the bulb creates a wave system that interferes with the hull wave system. The bulb produces a water system with smaller wave heights, which results in a smaller wave-making resistance, and consequently, in smaller total resistance (R_t). The wave-making resistance is defined as the resistance caused by waves while the ship is moving, while the wave resistance is caused by ocean waves hitting the hull [6]. A ship's speed, however, plays an important role in measuring the total resistance. The United States Naval Academy (2015) describes a ship's total resistance components in relation to the ship's speed, where the wave-making resistance (R_w) becomes more relevant as the ship's speed increases [7].

For a multi-pier bridge, it is important to determine if a bulb concept is viable, as in similar ship-related cases. The ship hull closest resembling a multi-pier bridge is a catamaran. Yun and Bliault (2012) studied the Small Water Plane Twin Hull Catamaran (SWATH), which is able to reach supercritical flow velocities. The authors found that for these ships, R_t marginally decreases when the ship is equipped with a bulbous bow [8]. The marginal R_t reduction is a consequence of two competing forces: viscous resistance (R_v) increases, while R_w decreases, due to the increase in bulb length. Moreover, Ghani and Wilson (2009) correlated the cross-section of a bulb (A_{BT}) to the bulb's wave horizontal size, a bulb's length (L_{PR}) to the bulb's wave phase in relation to the hull wave, and the volume of a bulb to the wave's amplitude (Table 1) [9]. Their findings provide guidance in sizing a bulbous pier.

Table 1. Bulb geometry parameters.

<table>
<tr><td>$C_{BB} = B_B/B_{MS}$</td><td>(1)</td><td rowspan="2">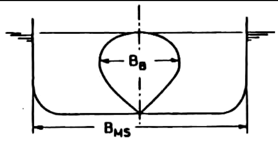
</td></tr>
<tr><td colspan="2">Breadth parameter (C_{BB}): The maximum breadth (maximum width of a bulb - B_B) of bulb area (A_{BT}) at the forward perpendicular, divided by the beam of a ship at amidships (B_{MS}).</td></tr>
<tr><td>$C_{LPR} = L_{PR}/L_{PP}$</td><td>(2)</td><td rowspan="2">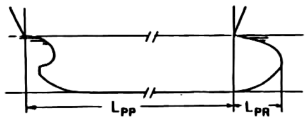
</td></tr>
<tr><td colspan="2">Length parameter (C_{LPR}): The protruding length (L_{PR}) divided by the length between perpendiculars (L_{PP}) of a ship.</td></tr>
<tr><td>$C_{ZB} = Z_B/T_{FP}$</td><td>(3)</td><td rowspan="2">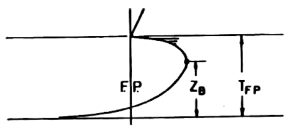
</td></tr>
<tr><td colspan="2">Depth parameter (C_{ZB}): The height (Z_B) of the foremost point of a bulb over the baseline divided by the draft (T_{FP}) at the forward perpendicular.</td></tr>
<tr><td>$C_{ABT} = A_{BT}/A_{MS}$</td><td>(4)</td><td rowspan="2">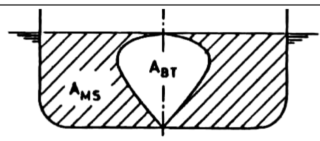
</td></tr>
<tr><td colspan="2">Cross-section parameter (C_{ABT}): The cross-sectional area (A_{BT}) of a bulbous bow at the forward perpendicular divided by a ship's midship section area (A_{MS}).</td></tr>
<tr><td>$C_{ABL} = A_{BL}/A_{MS}$</td><td>(5)</td><td rowspan="2">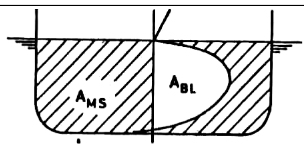
</td></tr>
<tr><td colspan="2">Lateral parameter (C_{ABL}): The area (A_{BL}) of a protruding bulb in the longitudinal plane divided by the midship section area of a ship (A_{MS}).</td></tr>
<tr><td>$C_{VPR} = \nabla_{PR}/\nabla_{WL}$</td><td>(6)</td><td rowspan="2">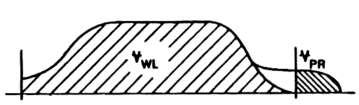
</td></tr>
<tr><td colspan="2">Volumetric parameter (C_{VPR}): The volume (∇_{PR}) of the protruding part of a bulb divided by the volume of displacement (∇_{WL}) of the ship. NOTE: Protruding is used here to mean that part of a bulb which extends in front of the forward perpendicular.</td></tr>
</table>

The previous studies on ship bulbs concluded that a bulbous bow reduces the R_t under similar conditions as a pier in an open channel. A long bulbous bow reduces a ship's non-dimensional maximum wave height (H_{nd}). The reduction of H_{nd} can be compared to a pier's wave ratio. Therefore, the bulb that causes more reduction in H_{nd} will be considered as the basis to determine initial bulbous pier geometry. This study focuses on pier wave height and splash reduction using a bulb attached to a bridge pier. The specific objectives of this research are as follows:

- Performing experiments in order to understand the impact of a bulbous on pier wave height;
- Developing an analytical model that predicts the effects of a bulbous pier on pier wave height based on the bulb's geometry and location.

2. Materials and Methods

2.1. Theoretical Formulation

A bulb wave (B_w) is the difference between non-bulb (PL_{nb}) and bulbous (PL_{bb}) pier water levels (Figure 4). A bulb can be analyzed as a standalone ship, where the bulb hull resistance is proportional to B_w. The addition of a bulb to a pier reduces pier wave height by removing energy from the water, thus making this energy unavailable to contribute to PL_{bb}.

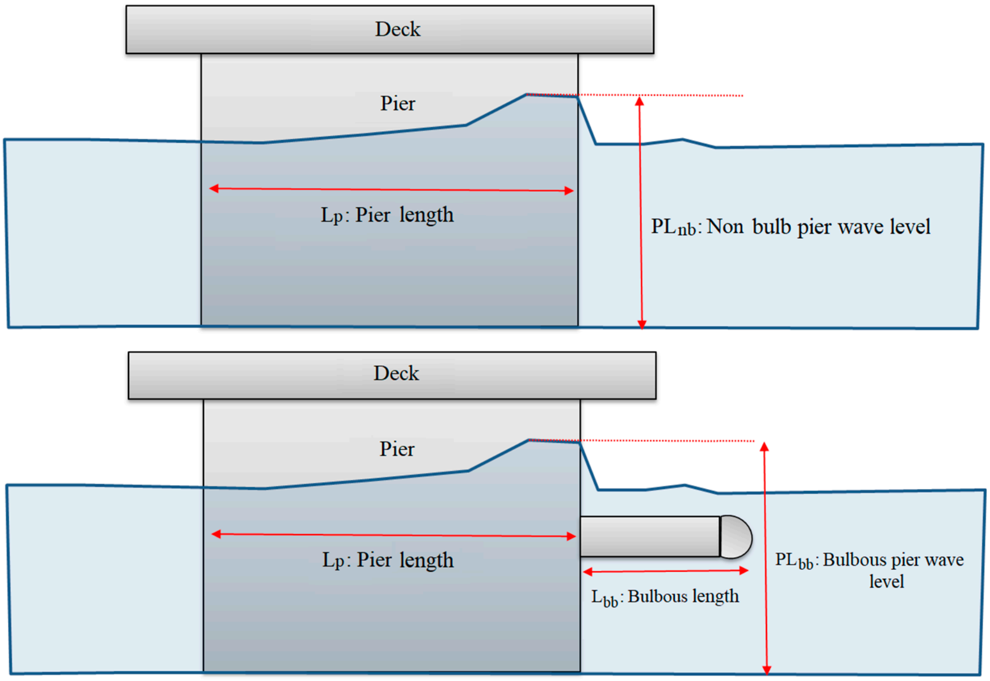

Figure 4. Pier with and without a bulb.

A ship moving through water is similar to a pier in an open channel. They both create waves as the water moves around them. According to ship wave theory, the energy in a wave is proportional to the square of the wave height [10]. Therefore, if the wave height doubles, the energy required for wave-making becomes four-fold (Equation (7)). This is the reason that wave-making is the main component of a ship's total resistance.

In ship design, R_w becomes more important than the R_v when a ship's wavelength reaches a value equal to the ship's length. The bulb wavelength (L_w) is defined by Equation (8) [10]:

$$R_w = f\left(C_w, v^4\right) \tag{7}$$

$$L_w = \frac{2\pi v^2}{g} \tag{8}$$

where v is the flow velocity, g is the gravity acceleration, and C_w is the wave-making coefficient. Since B_w is a consequence of a bulb's total resistance, an increase in the magnitude of B_w will be directly related to a decrease of the PL_{bb} and, as a consequence, to a decrease in deck splashing. The power required to move a ship is directly related to the total hull resistance; the hull resistance is the force that the ship experiences opposite to the motion of the ship as it moves. The total hull resistance (R_t) has three main components:

$$R_t = R_v + R_w + R_a \tag{9}$$

where R_t is the total resistance (in pound force), R_v is the viscous resistance, R_w is wave-making resistance, and R_a is the air resistance. In piers, the air resistance is negligible; thus, Equation (9) can be rewritten as:

$$R_t = R_v + R_w \tag{10}$$

The total bulb resistance can be calculated as:

$$R_t = 0.5\rho BB_{as}(C_v + C_w)v^2 \tag{11}$$

where BB_{as} is the submerged bulb area, and C_t is the total resistance coefficient (C_t = C_v + C_w). Moreover, C_{vt} can be defined as:

$$C_{vt} = \frac{0.075}{\log 10(Re - 2)^2} \tag{12}$$

where C_{vt} is the viscous resistance tangential to the bulb, and R_e is the Reynolds number.

$$Re = \frac{vL_{bbs}}{k} \tag{13}$$

where L_{bbs} is the submerged bulb's length, and k is the kinematic viscosity ($1.2260{*}10^{-5}$ ft^2/s for fresh water). Therefore, C_v will be:

$$C_v = C_{vt} + C_{vt}k_n \tag{14}$$

where k_n is the viscous perpendicular resistance coefficient, and is defined as:

$$k_n = 12\left(\frac{V_{bb}}{Y_s}\frac{B_d}{L_{bbs}}\right) \tag{15}$$

where V_{bb} is the bulb's volume, B_d is the bulb's diameter, and Y_s is the bulb's submerged depth. For the same testing conditions (flume flow and flume slope), attaching the bulb to a pier changes the water's velocity. The PL_{nb} can be calculated using Equation (16) (total energy equation). Equation (16) assumes that the water's energy will be transferred to the pier wave and then into PL_{nb}.

$$PL_{nb\_calc} = E = y_h + \frac{V^2}{2g} \tag{16}$$

where E is the total energy, Y_h is the hydraulic depth in ft., v is the water velocity, and g is gravity acceleration.

Since B_w is a function of R_t, it shall have two components:

$$B_w = B_{wv} + B_{ww} \tag{17}$$

where B_{wv} is the viscous bulb wave, and B_{ww} is the wave-making bulb wave. Since the bulb takes energy from the flow, the flow velocity at the end of the bulb will be less than the channel flow velocity. This reduced velocity is responsible for B_{wv} and B_{ww}. The practical bulbous lengths are not long enough to reach the bulb's wavelength values, making the viscous resistance the dominant component. To transfer the bulbous pier model's dimensions into a full-size bulbous pier, the following rules apply:

- The Froude number of the model (Fr_m) is the same as the Froude number of the flow around the pier (Fr_p).
- The wave-making coefficient of the bulb model (C_w) and the bulb (C_{wp}) are the same.

Viscous Resistance Error

In a ship, the use of the Froude number to scale the model to a full-size bulb introduces a great deal of error—mostly regarding viscous resistance—due to the fact that the water density cannot be scaled [11]. The theory on viscous resistance error mitigation in ships assumes that the force applied to the hull is parallel to the ship's waterline. This is not the case in bulbous piers, where the pier under the bulb creates forces perpendicular to the bulb, and in the opposite direction to the water flow. One method to mitigate the viscous resistance error is to increase the model's surface roughness. In this study, in the bulb model, the surface roughness was increased in a 3D-printed model, with layers perpendicular to the flow. The proposed full-size bulb was built out of commercial steel pipe with a Manning's roughness coefficient of 0.012 because the closest material to the 3D-printed model was a corrugated pipe with a Manning's roughness coefficient of 0.022.

2.2. Bridge Selection

Since splashing was observed in the Broadbent Boulevard box culvert at Duck Creek, Las Vegas, during flash floods, this bridge was selected to evaluate the applicability of the bulbous pier concept (Figure 5). Table 2 shows some information on the flow, pier, and channel geometry provided by the Clark County Regional Flood Control District [12].

A comparison between the water velocity around Duck Creek Bridge pier and that of high-speed ships indicated that a bulbous pier falls into the speed ranges used for a bulbous bow. Table 3 compares speeds and Froude number values for high-speed ships and the water velocity around Duck Creek Bridge pier in Las Vegas, Nevada.

Figure 5. Duck Creek flood channel, Las Vegas metropolitan area.

Table 2. Duck Creek Channel and bridge dimensions.

Channel	
Parameter	Value
Width (ft.)	118.00
Height (ft.)	5.70
Length (ft.)	500.00
Flow Velocity (ft./sec.)	20.14
Submerged Height (ft.)	5.00
Hydraulic Depth (ft.)	5.00
Submerged Area (ft.^{2})	590.00
Bridge	
Pier Height (ft.)	5.70
Pier Hydraulic Depth (ft.)	5.00
Pier Length (ft.)	152.43
Pier Width (ft.)	1.50
Pier Nose Radius (ft.)	1.50
Pier Submerged Area (ft.^{2})	7.50

Table 3. Froude number calculation for high-speed ships and Duck Creek Bridge Pier in Las Vegas, Nevada.

Ships/Bridge	Fr	v (ft./sec.)	L (ft.)
USS Sea Fighter (FSF-1)	1.06	92.83	239.5
USS Swift (HSV-2)	0.75	75.95	321
USS Independence (LCS 2)	0.62	72.00	418
Duck Creek Bridge Pier	0.31	22.00	152

2.3. Flume Testing Plan

The experimental tests were performed in a flume at the University of Nevada Las Vegas (UNLV), and the test plan consisted of the following phases:

1. Verifying the flume Manning's roughness coefficient
2. Obtaining the bulb optimal submerged depth
3. Testing twelve bulb models for eight steady-state conditions in the flume (slope and the pump RPM), with the maximum hydraulic depth (Y_h) of 0.375′

The UNLV flume instrumentation consisted of a pump RPM meter, a flume slope meter, and a magnetic flow meter located in the pipe feeding the flume. For the bulbous pier testing, new instrumentations were added to the flume:

- An Endress + Hauser Liquicap capacitive level meter Liquidcap T FMI21; this equipment measured the pier level (PL_{nb}, PL_{bb}) (Figure 7).
- A Greyline area velocity flow meter, model AVFM 5.0; this equipment measured the flume flow rate (Q), velocity (v), and hydraulic depth (Y_h). The instrument was located at the bottom of the flume in front of the pier nose, a few inches away from the bulb (Figure 6).
- A Measurement Computer USB-1608G Data Logger; this data logger collected the data coming from the pipe flow meter and level meter, as well as the three outputs from the AVFM 5.0: water velocity, water level, and flow rate.
- To scale, display, and record the data collected by the data logger, the Measurement Computer DasyLab application was used, and the data collected were stored in Excel CSV format.

Froude number, bulb submerged length, bulb submerged area, and other values were calculated in an MS Access database.

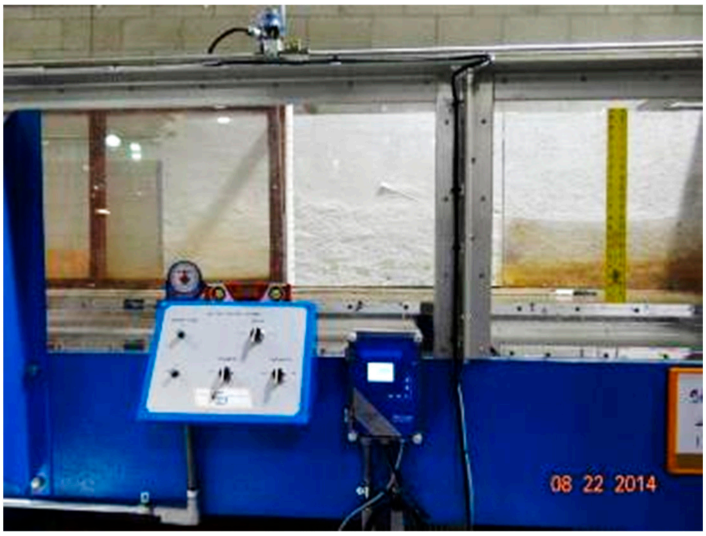

Figure 6. Greyline AVFM 5.0 installed on the flume.

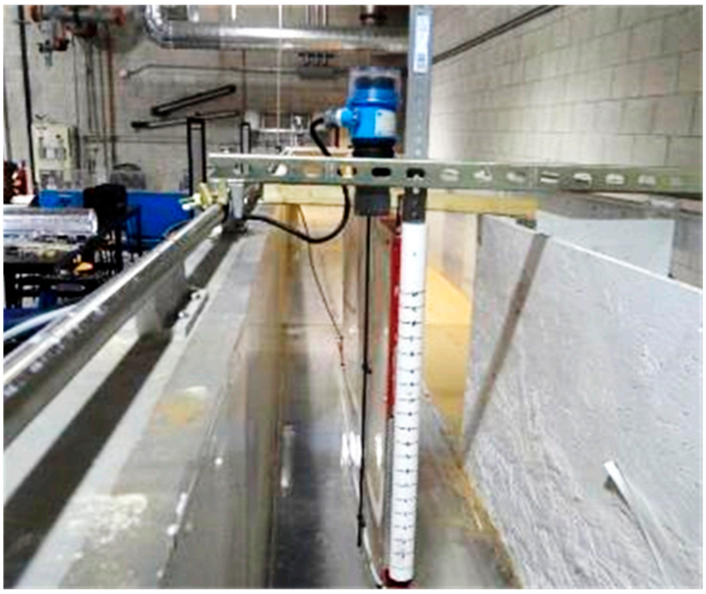

Figure 7. Level meter location in the flume.

2.3.1. Verifying the Manning's Roughness Coefficient

For any flow condition in the flume, the Manning's roughness coefficient converged to a single number of n = 0.010.

2.3.2. Optimal Bulb Submerged Depth

From the literature review, the optimal bulb submerged depth (Y_s) was determined by running the flume at maximum flow and changing Y_s. Preliminary tests showed that optimum Y_s occurred when half of the bulb's diameter was submerged.

2.3.3. Steady-State Test Matrix

In order to evaluate the pier water level reduction produced by the bulb, a pier model was placed into a hydraulic flume and tested. Two sets of data were collected: one from the pier, and the other for the pier with the bulb. The flume running at a predetermined Y_h is called *steady-state* in this paper. This is different from the actual behavior of open channels, where Y_h changes as flow conditions change.

The test matrix (Table 4) contains eight flume set points (slope and the RPM), where $Y_h = 0.375'$. Twelve bulb models were selected for each flume set point. The bulb models were divided into four lengths and three angles. Bulb length was measured at the upper side of the bulb. The bulb angle was the angle between the bottom of the flume and the bottom of the bulb.

Table 4. The test matrix.

Independent Variables	Value	Units	Condition
Pump Speed, Flume Slope (eight cases, $Y_h = 0.375$)	(550, 1.24), (601, 1.59), (568, 1.99), (570, 2.38), (630, 2.78), (714, 3.16), (750, 3.59), and (765, 4.26)	RPM, %	$Y_h = 0.375$
Bulbous Horizontal Upper Length	0.67, 0.96, 1.25, 1.54, and 1.83	ft.	-

2.4. Flume Capabilities

Table 5 shows the flume characteristics used at UNLV.

Table 5. Flume characteristics.

Characteristic	Values	Unit
Pump Nominal Speed	1185	RPM
Pump Nominal Flow	3600	GPM
Flume Pump Max. Speed	980	RPM
Manning's Coefficient (n)	0.010	-
Flume Width	1.5	ft.
Flume Length	58	ft.
Flume Max. Slope	4.1	%
Flume Min. Slope	0	%

2.5. Dimensional Analysis

For a flume with its width restricted to 1.5′ and running at Fr = 1.59, the Y_h is equal to 0.58′. The model was scaled down using the Froude number, and a model scale factor of 0.12 was obtained. For the experimental flume runs, a Y_h equal to 0.375′ was selected to allow for a larger number of supercritical set points. This hydraulic depth also provided room for the expected increase in Y_h due to the introduction of the bulb. The result of the dimensional analysis is shown in Table 6. Since the pier height does not have any significance in the equation governing bulb design, it was increased to 2′ to accommodate the necessary instrumentation.

Table 6. Flume and pier model dimensions.

	Parameter	Value
Flume	Width (ft.)	1.50
	Height (ft.)	1.67
	Length (ft.)	25.00
	Flow Velocity (ft./sec.)	6.88
	Submerged Height (ft.)	0.58
	Hydraulic Depth (ft.)	0.58
	Area (ft.^{2})	2.50
Pier Model	Pier Height (ft.)	0.67
	Pier Submerged Height (T_{FP}) (ft.)	0.58
	Pier Length (L_{PP}) (ft.)	2.00
	Pier Width (B_{MS}) (ft.)	0.17
	Pier Submerged Area (A_{MS}) (ft.^{2})	0.10
	Pier Height (V_{WL}) (ft.)	0.67

2.6. Bulbous Pier Geometry

The pier model dimensions were selected using suggested values for bulb dimensions from Ghani (2009) [9]. The width of the bulb was set to be the same as the pier width. Table 7 shows the bulbous pier geometric characteristics.

Table 7. The bulbous pier geometric characteristics.

Parameter	Min.	Max.	Unit	Abbreviation
Diameter	0.17	0.17	ft.	B_B
Length	0.03	0.13	ft.	L_{PR}
Area	0.16	0.40	ft.^{2}	-

3. Results and Discussion

3.1. Pier Water Level and Bulbous Pier Water Level

The experimental results showed that the bulb decreased the pier's water level. The two-sample t-tests, for PL_{nb} and PL_{bb}, showed that the bulbous pier's average water level was less than the non-bulb pier (see Appendix A).

3.2. Initial Assumptions

The initial bulb length (L_{bb}) values, derived from Ghani's (2009) design parameter values, proved to be insufficient to produce a significant reduction in the pier wave ratio (PWR). The short bulb with a 0° pitch angle had a spraying problem. Water over the bulb tip detached from the flow and sprayed over the pier (Figure 8). To avoid this problem, the L_{bb} would have to be extended to lengths not suitable for construction, somewhere between 10′ and 12′. The initial assumption that the L_{bb} is directly related to the PWR was confirmed (Figure 9). A higher PWR indicated that the PL_{bb} was lesser than the PL_{nb}.

To correct the spraying problem, the bulbous pitch angle was increased to 5° and 10°. The pitch angle is defined as the angle between the bulb's horizontal axis and the bottom of the flume. The selection of the pitch angle was based on the C_{ZB} value, used by Ghani and Wilson (2009), and Table 8 [9]. A C_{ZB} = 0.329 is between a 5° and 10° offset between the tip of the bulb and the top of the bulb (Figure 10), depending on the length of the bulb.

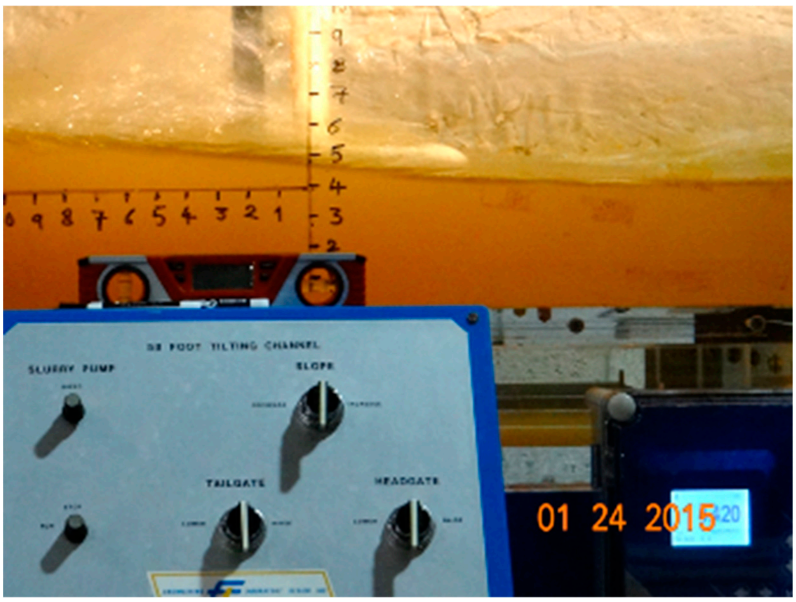

Figure 8. Bulbous pier spraying problem.

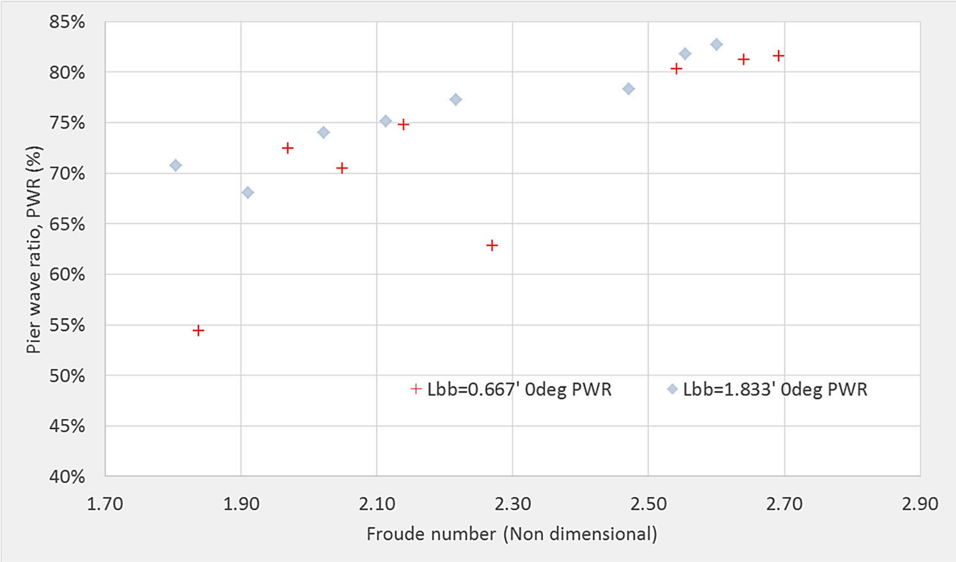

Figure 9. Pier wave ratio for 0° pitch angle bulb, L_{bb} = 0.667′ and 1.833′.

Table 8. Pier model dimensions.

Dimension	Value	Unit	Scale	Abbreviation
Pier Height	0.67	ft.	0.12	-
Pier Submerge Height	0.58	ft.	0.12	T_{FP}
Pier Length	2.00	ft.	0.12	L_{PP}
Pier Width	0.17	ft.	0.12	B_{MS}
Pier Submerge Area	0.10	ft.	0.12	A_{MS}
Pier Height	0.67	ft.	0.12	V_{WL}

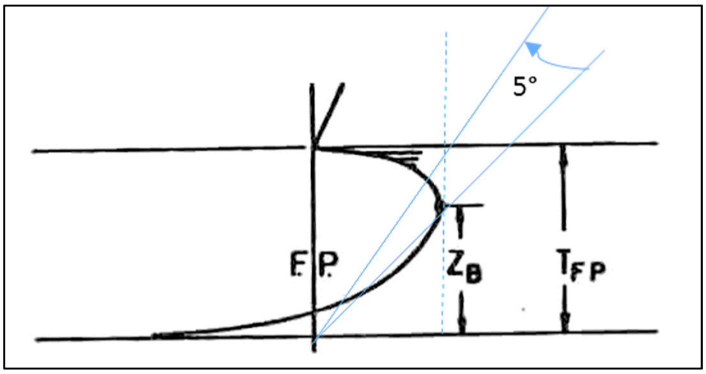

Figure 10. Bulb C_{ZB} interpretation.

The increase in the pitch angle was accomplished by rotating the 0° bulb, having the upper part of the bulb-pier intersection as a fixed point. The introduction of the pitch angle corrected the spraying problem and increased the PWR for the bulb with the same upper horizontal length (Figure 11). The results also showed that an increase in the pitch angle reduced the PL_{bb} by eliminating the flow over the bulb (Figure 12).

For the bulbs with 5° and 10° pitch angles, the bulbous submerged length was the bulbous length at the waterline level (L_{bbs}). The reduction in L_{bbs} due to the introduction of the pitch angle decreased PL_{bb} (Figure 13), but provided the opportunity to brace the bulb tip to the pier once the tip cleared the water line. The 0° pitch angle bulb was discarded because of the large L_{bbs} required to eliminate the spraying problem.

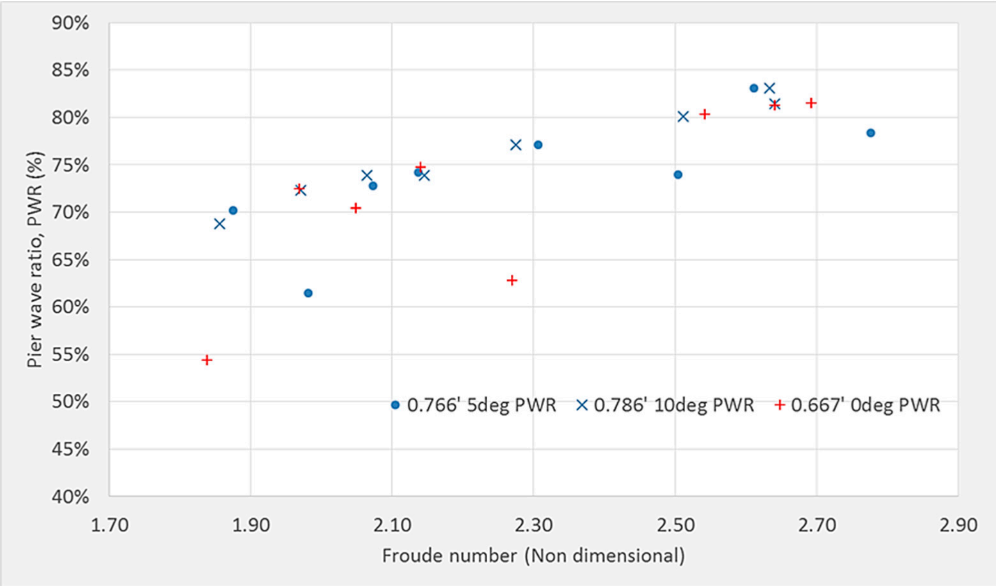

Figure 11. PWR for bulbs with different pitch angles.

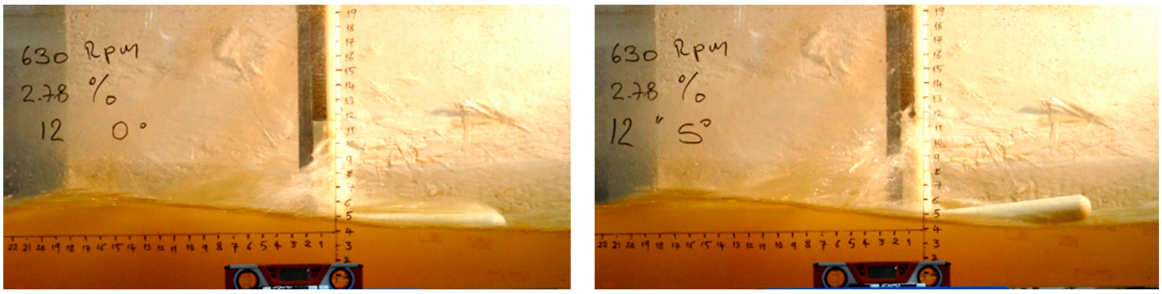

(**a**) (**b**)

Figure 12. Bulbs spraying problem, at (**a**) 0°, and (**b**) 5° pitch angles.

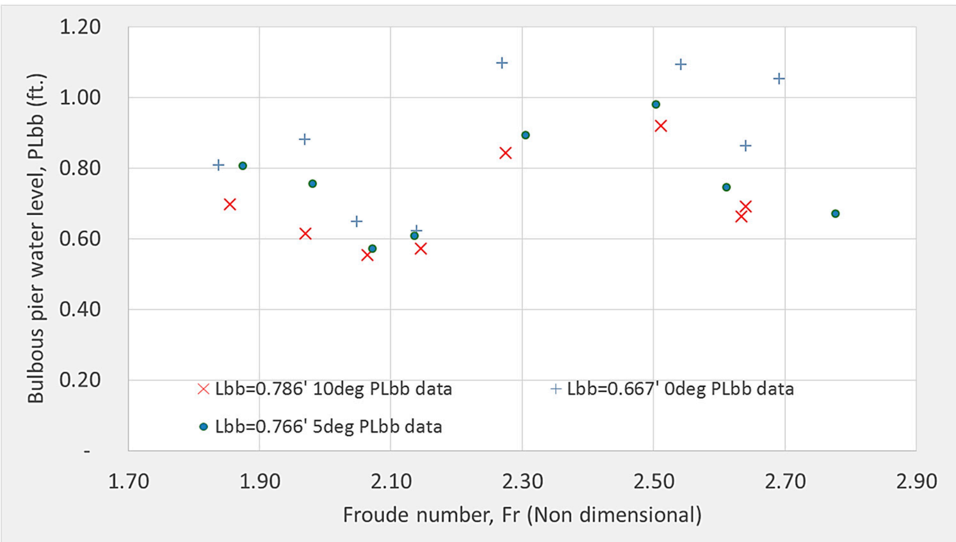

Figure 13. PL_{bb} with similar horizontal upper length, at 0°, 5°, and 10° pitch angles.

3.3. Bulbous Pier Water Level

According to Figures 14–16, the use of Equation (16) overestimates the value of the calculated non-bulb pier water level (PL_{nb_calc}) vs. the data collected for the non-bulb pier water level (PL_{nb_data}). This error propagates to the calculation of the theoretical bulbous pier water level (PL_{bb_calc}). The overestimation is a consequence of energy losses due to frictional losses at the pier nose, and the air-water interactions ignored by Equation (16).

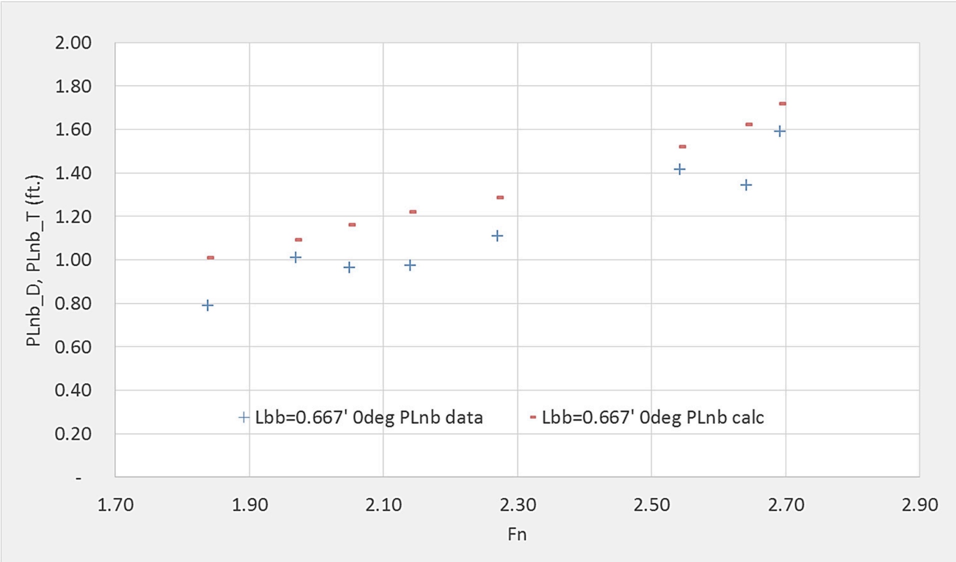

Figure 14. PL_{nb_data} and PL_{nb_calc} for bulbs with 0° pitch angle.

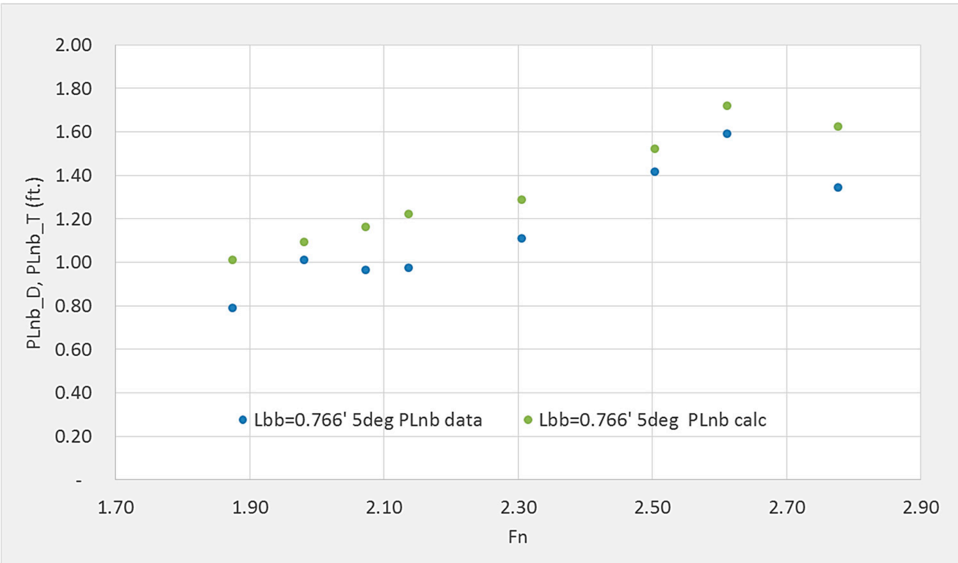

Figure 15. $PL_{bb-data}$ and $PL_{bb-calc}$ for bulbs with 5° pitch angle.

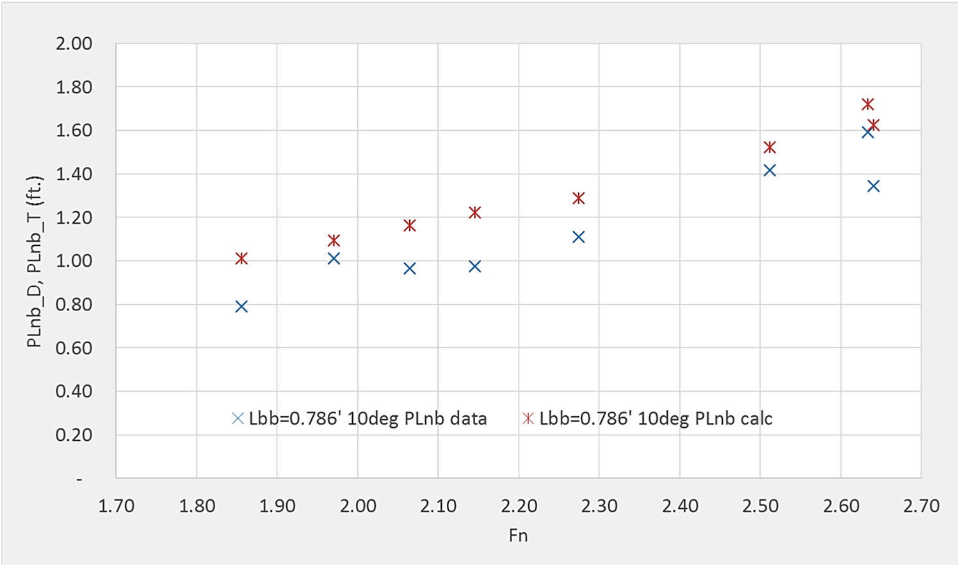

Figure 16. PL_{bb_data} and PL_{bb_calc} for bulbs with 10° pitch angle.

3.4. Bulb Wave

B_w follows the form of the hull resistance curve as predicted (Figures 17 and 18). Consequently, R_v, and R_w can be calculated using the proposed set of equations for PL_{bb}.

For the 10° bulbous with an L_{bb} over 0.995′, the L_{bb} is meaningless; since once the bulbous tip is above the water, there is no contribution to the L_{bbs}. Reading the PL_{bb} using the capacitive level meter had a large standard deviation, as a consequence of the turbulent nature of the pier wave. To simplify the mathematical analysis, the PL_{bb} maximum was selected to calculate the B_w. This assumption was in line with the goal of preventing deck splashing.

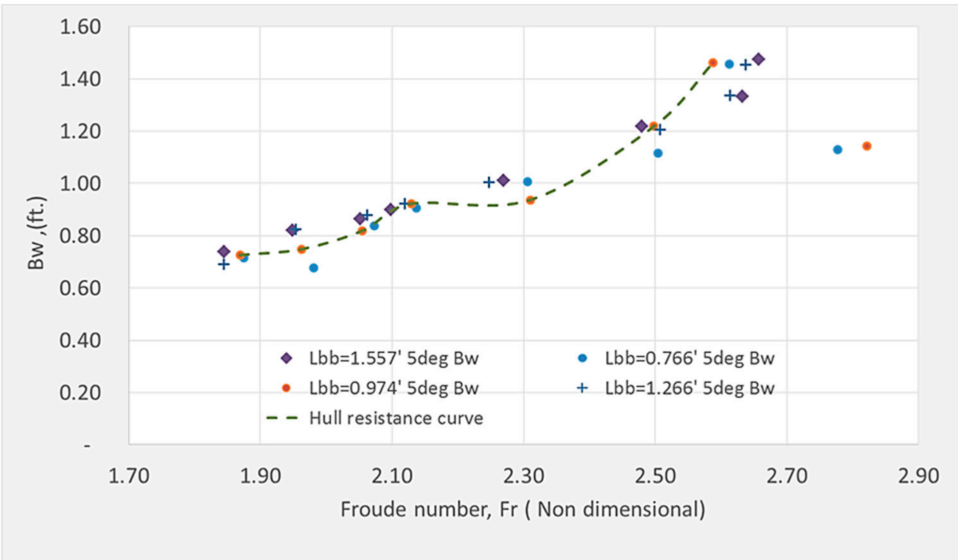

Figure 17. B_w for 5° pitch angle.

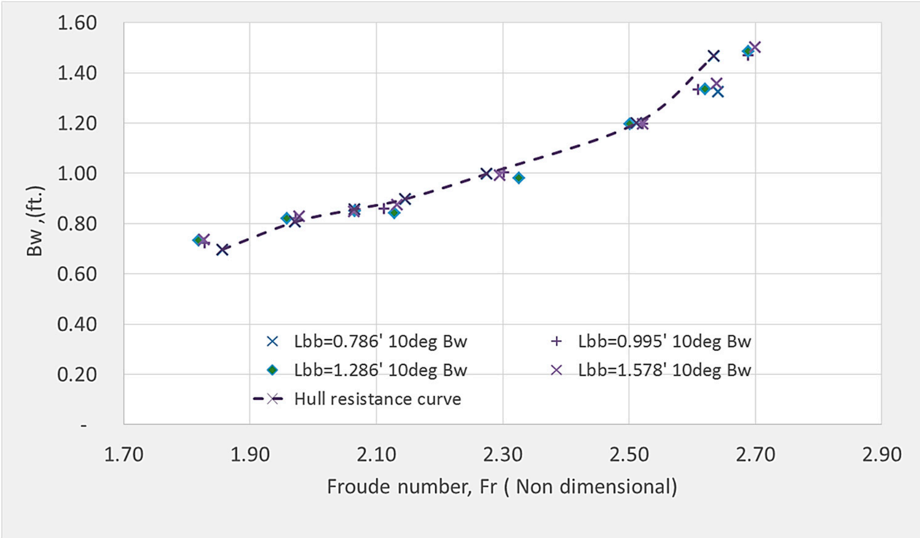

Figure 18. B_w for 10° pitch angle.

3.5. Bulbous Viscous and Wave-Making Resistance

The Y_h in the flume changed constantly due to the turbulent nature of the flow. Changes in the Y_h affect the calculation of the BB_{as}, and attempts to reduce the flow turbulence, while maintaining high water velocity, were unsuccessful. The data recording system stored over 3000 points for the test case; therefore, a narrow range of Y_h ($4.4 < Y_h < 4.6$ in.) was selected to obtain a statistically significant number of readings per test case ($n > 30$).

From Figures 19–21, it is clear that the viscous resistance was the main component of the B_w. According to ship hull design theory, the wave-making resistance becomes dominant when the L_{bbs} is equal or greater than the L_w. For the 0° pitch angle bulb, the submerged length was always less than the bulb wavelength (see Equation (18) and Figure 19). Consequently, Equation (17) was modified to include only the viscous component (Equation (19)). This assumption underestimates the value of the B_w at lower Fr numbers, where the bulb wavelength is closer to the L_{bbs}.

$$L_b = L_w = \frac{2\pi v^2}{g} \tag{18}$$

$$B_w = B_{wv}. \tag{19}$$

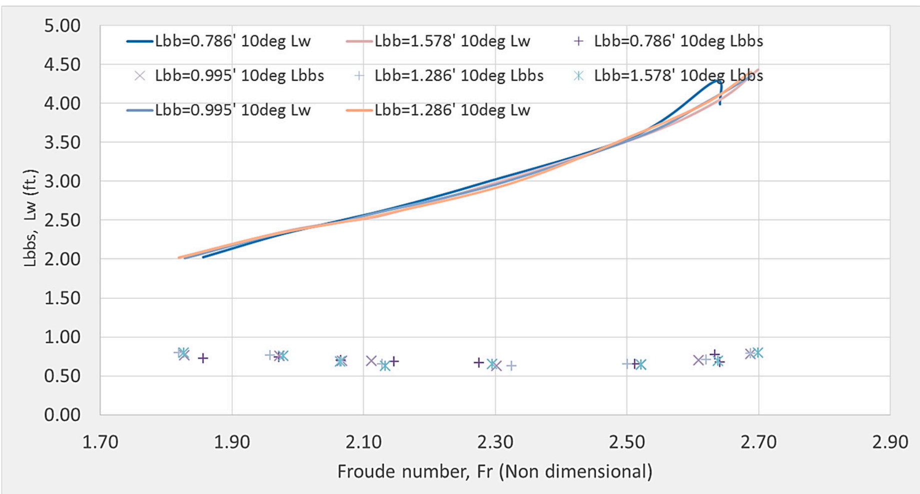

Figure 19. L_{bbs} and L_w, at 5° pitch angle.

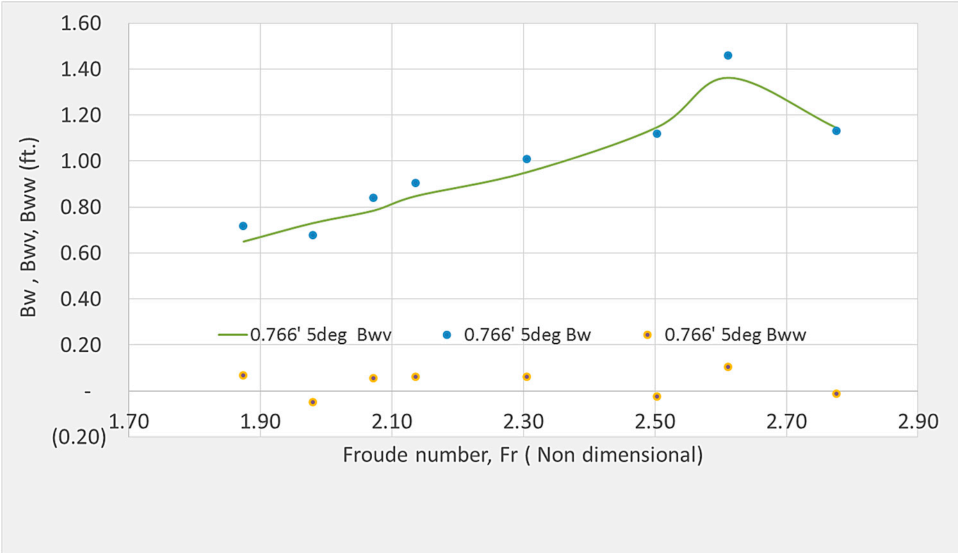

Figure 20. B_w, B_{wv} and B_{ww} for the bulbous pier with 5° pitch angle.

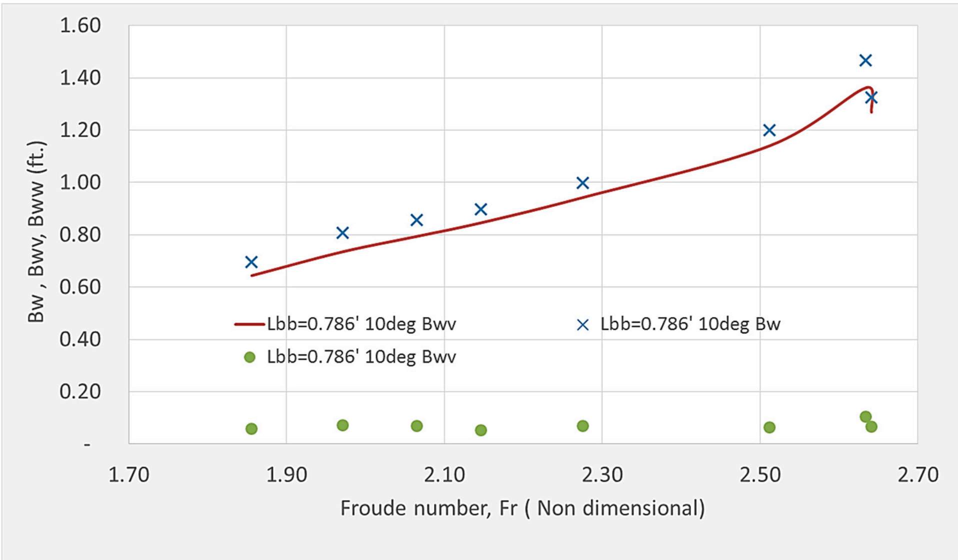

Figure 21. B_{wv} and B_{ww} for the bulbous pier with 10° pitch angle.

This approach will eliminate the need for modeling each bulbous pier to obtain the B_{ww}. The cost of modeling a bulbous pier in a flume can easily exceed the cost of building a pier extension.

3.6. Pier Wave Level Ratio (PWR)

The proposed equation to calculate the pier wave ratio (PWR_{calc}) closely matches the experimental values (PWR_{data}). Figures 22 and 23 compare the values of PWR_{data} vs. PWR_{calc}. The PWR_{calc} is more accurate for the bulbs with pitch angles of 5° and 10°; this is a consequence of the elimination of the water flowing over the bulbous for the 0° pitch bulb.

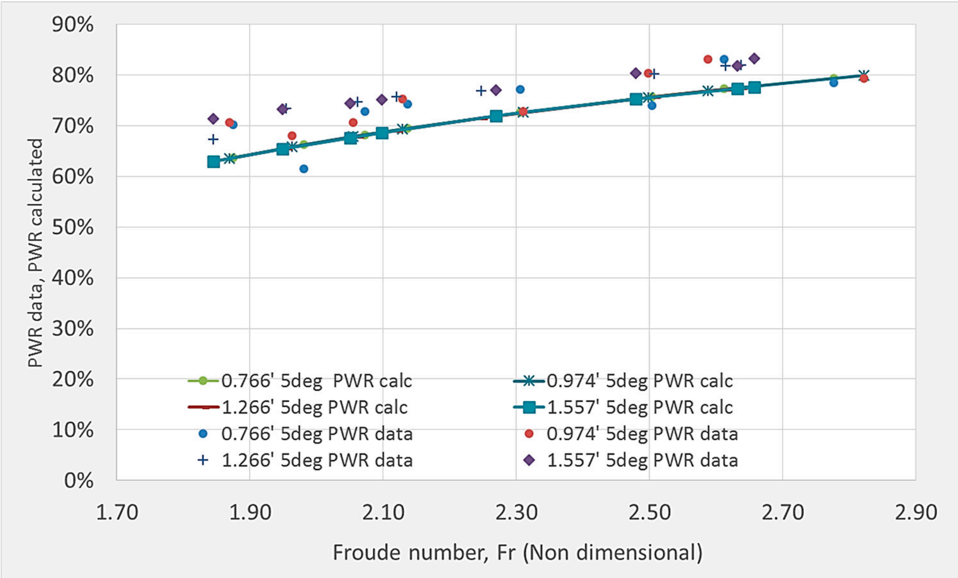

Figure 22. PWR_{data} vs. PWR_{calc}, bulbous pier with 5° pitch angle.

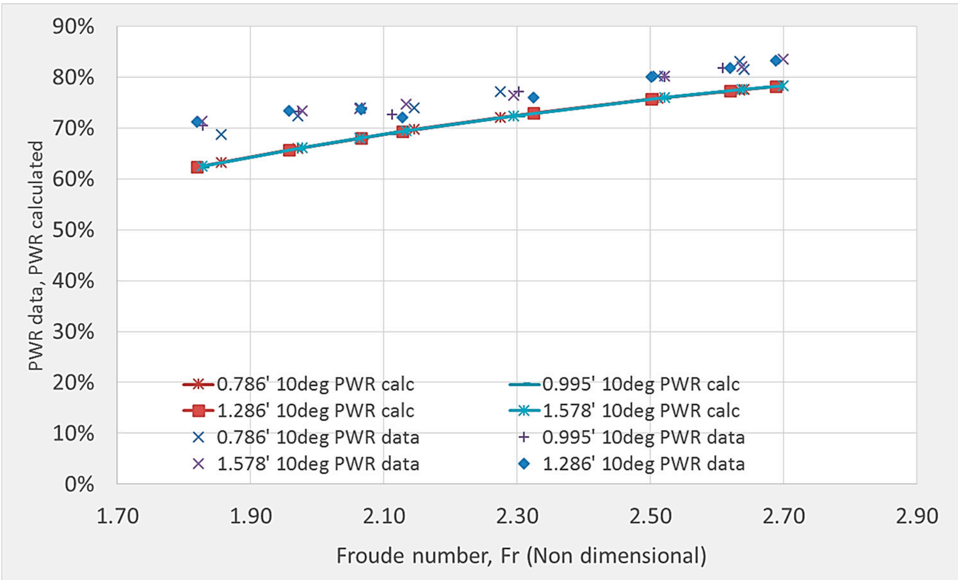

Figure 23. PWR_{data} and PWR_{calc} vs. Froude number (F_r), bulbous pier with 10° pitch angle.

3.7. Design Curves for Pier Wave Reduction

The experimental results showed that the bulb's tip should be above the water level to prevent deck spraying. Consequently, $L_{bb} < 0.9'$ should be ignored. For $L_{bb} > 1.2'$, an additional bulb length, above the water level, does not contribute to the PWR. Only two bulbs met these restrictions: $L_{bb} = 0.974'$ at 5°, and $L_{bb} = 0.786'$ at 10°. In order to translate the experimental results into a full-size bulb, the L_{bb} in the PWR vs. the Froude number charts, is normalized by dividing the L_{bb} by the Y_s; Figure 24 shows how the L_{bb} and Y_S are measured in a bulb. The Y_s is based on the condition that the bulb will only be submerged up to the bulb's longitudinal centerline.

The decision between using the 5° or the 10° bulb requires full-size testing to evaluate the residual spaying problem detected in the 10° bulb, and the deflection problem associated with a long bulbous (5°). Figures 25 and 26 show the normalized relations for the two bulbs.

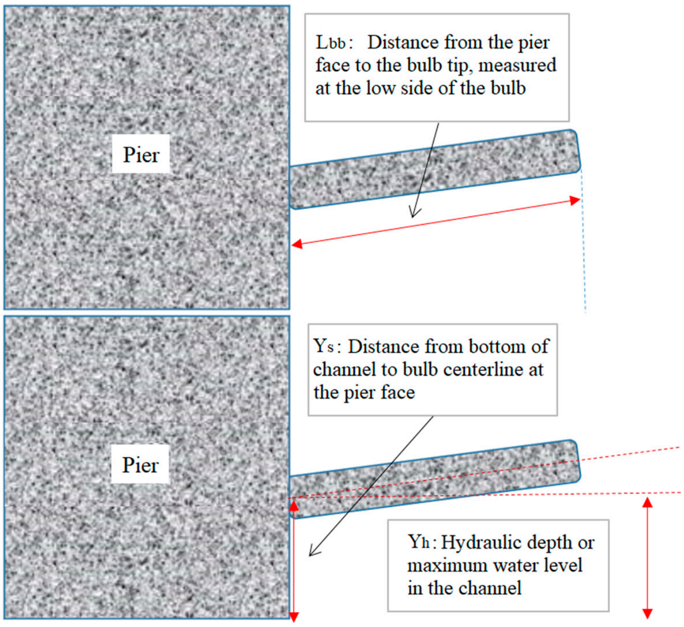

Figure 24. Normalized parameters' description.

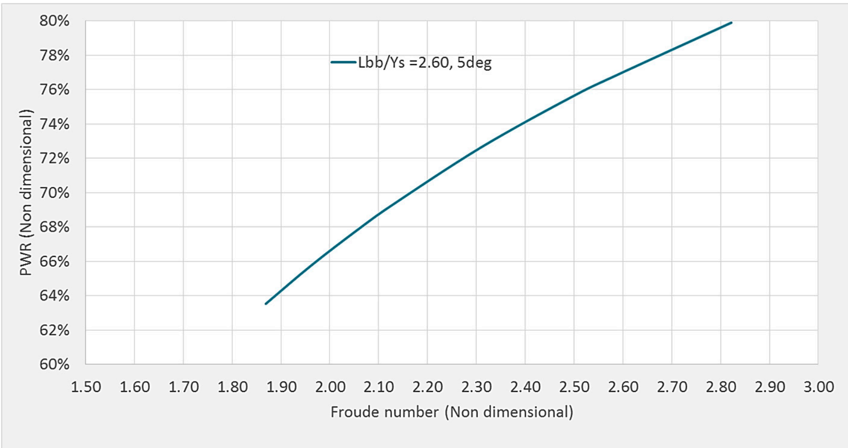

Figure 25. Proposed PWR approximation using normalized bulb length, 5° pitch angle, L_{bb} = 0.974′, Y_s = 0.375′.

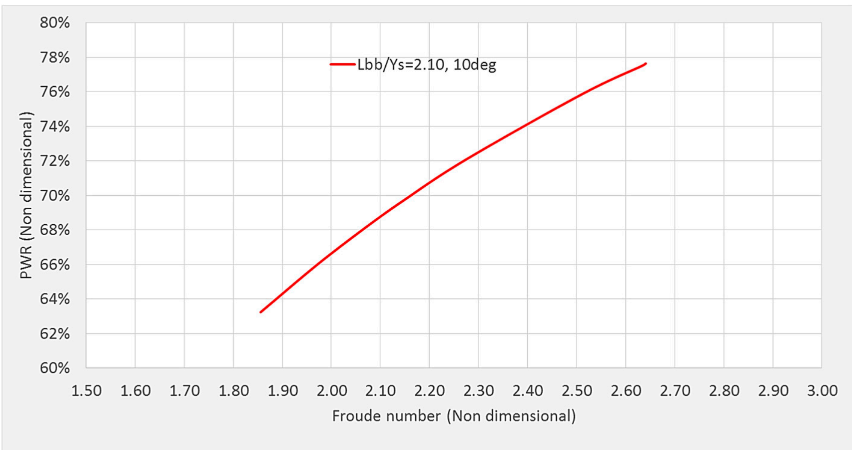

Figure 26. Proposed PWR approximation using normalize bulb length, 10° pitch angle, L_{bb} = 0.786′, Y_s = 0.375.

3.8. Flow Behavior After the Pier-Bulb Intersection

The analysis of the water level after the bulb-pier intersection was not the subject of this research, but the reduction of the water level for the bulbous pier case is a factor to consider in the selection of bulbous pier length. Table 9 illustrates the changes in the flume water levels after the bulbs were added. For most cases, the addition of a bulb reduces the water level for Froude numbers under 2.5, and maintains the flume water level for Froude numbers larger than 2.5. This can be attributed to a reduction in the water turbulence produced by the bulb (Figure 27).

Table 9. Water level after the bulb.

Pump Speed (RPM)	Flume Slope (%)	Pitch Angle (deg.)	Bulb Length (ft.)	Froude Number	Water Level (in.)
550	1.24	0	-	1.85	7.0
550	1.24	0	1.25	1.80	5.5
550	1.24	5	1.27	1.84	6.0
550	1.24	10	1.29	1.81	6.0
568	1.99	0	-	2.05	5.5
568	1.99	0	1.25	2.03	5.0
568	1.99	5	1.27	2.06	5.0
568	1.99	10	1.29	2.06	5.0
570	2.38	0	-	2.13	5.1
570	2.38	0	1.25	2.10	5.2
570	2.38	5	1.27	2.11	5.0
570	2.38	10	1.29	2.12	5.0
601	1.59	0	-	1.97	8.0
601	1.59	0	1.25	1.94	7.5
601	1.59	5	1.27	1.95	7.0
601	1.59	10	1.29	1.95	6.8
630	2.78	0	-	2.25	8
630	2.78	0	1.25	2.26	6.5
630	2.78	5	1.27	2.24	6.5
630	2.78	10	1.29	2.31	6.0
714	3.16	0	-	2.49	6.0
714	3.16	0	1.25	2.52	6.0
714	3.16	5	1.27	2.50	6.0
714	3.16	10	1.29	2.49	6.0
750	3.59	0	-	2.59	5.5
750	3.59	0	1.25	2.58	5.5
750	3.59	5	1.27	2.60	5.5
750	3.59	10	1.29	2.60	5.5
765	4.26	0	-	2.70	4.5
765	4.26	0	1.25	2.63	5
765	4.26	5	1.27	2.63	4.5
765	4.26	10	1.29	2.68	4.5

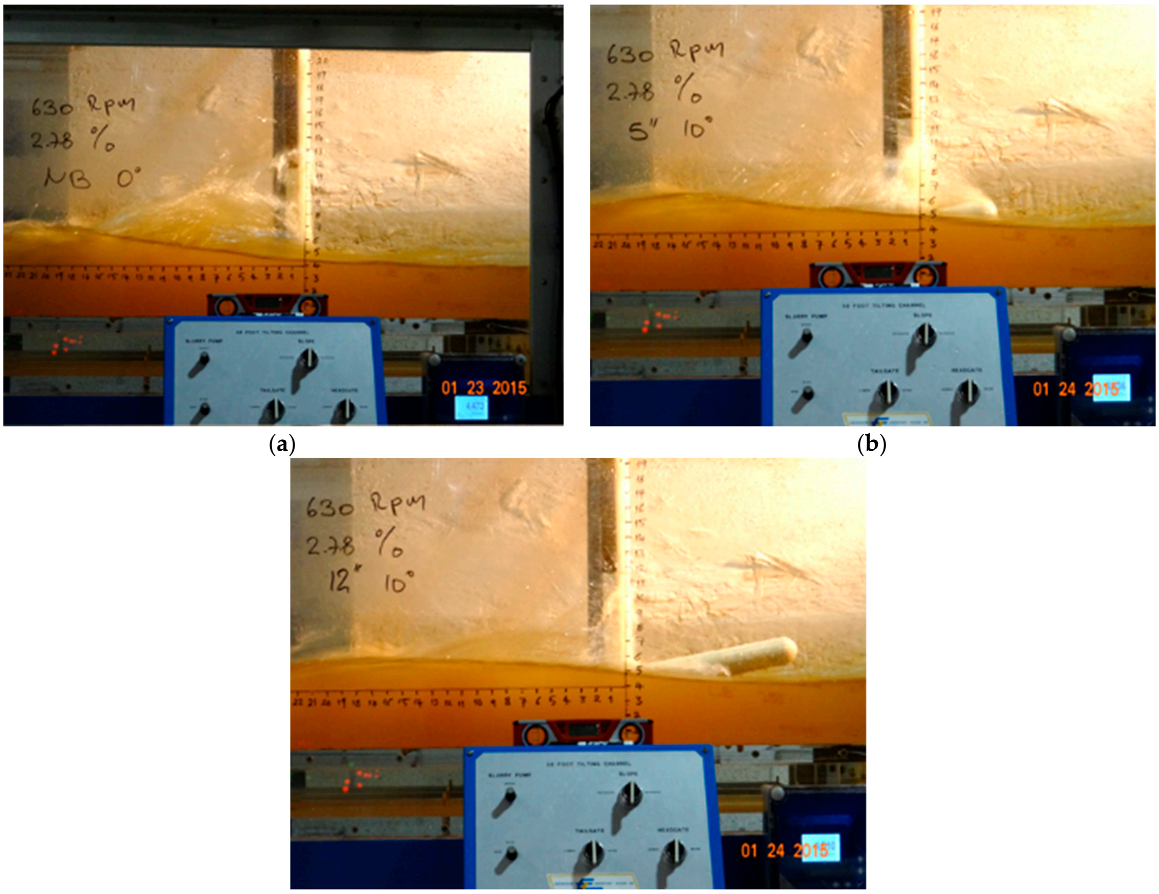

(a) (b) (c)

Figure 27. Water level after the pier-bulb intersection for (**a**) non-bulb pier, (**b**) bulbous pier with L_{bb} = 5″ and at 10° pitch angle, and (**c**) bulbous pier with L_{bb} = 12″ and at 10° pitch angle.

3.9. The Bulbous Pier vs. the Pier Extension

A pier extension is designed and built for a specific range of flow conditions. If the open channel network is modified and the flow conditions change, the pier extension needs to be modified, most likely increased in length. The increase of length in a pier extension is not a desirable outcome because every square foot of pier extension increases the energy subtracted from the flow. This energy subtraction may transform the flow from supercritical to subcritical, and have undesirable outcomes. A bulbous pier's smaller area subtracts less energy from the flow, allowing a wider set of flow conditions.

4. Proposed Pier Bulbous Design Method

For a given open channel with a pier, the following method is proposed:

a. Determine the open channel water depth (Y_h) via field data or open channel equations;
b. The optimal bulb submerged depth (Y_s) is equivalent to the maximum hydraulic depth (Y_h) at bulb centerline, see Figure 30;
c. The bulb diameter shall be equal to the pier width;
d. Determine the non-bulb pier wave height using the following equation or field value:

$$PL_{nb\ calc} = E = y_h + \frac{V^2}{2g}$$

e. Calculate the open channel Froude number (F_r);

f. Using Figure 28 or Figure 29, determine the L_{bb}/Y_s for the Froude number calculated in the previous step;

g. Calculate the bulb length using Y_s equal to Y_h;

h. Verify whether the PWR reduces the pier wave to an acceptable level; if not the cylindrical bulbous is not a solution. In order to increase the PWR, the bulb submerged area needs to be increased, which leads to a different bulb shape, which is a subject of further research.

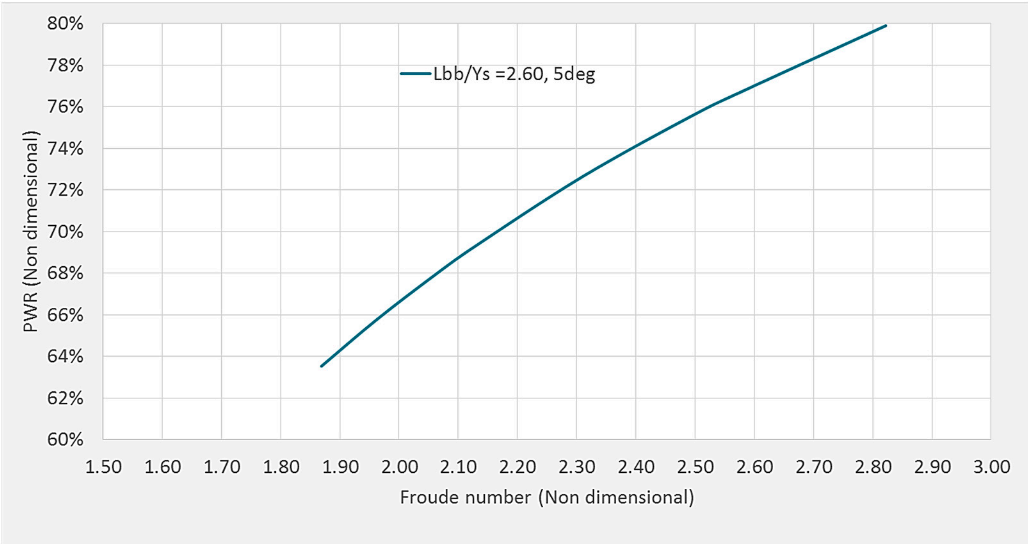

Figure 28. Proposed PWR approximation using normalized bulb length, and 5° pitch angle.

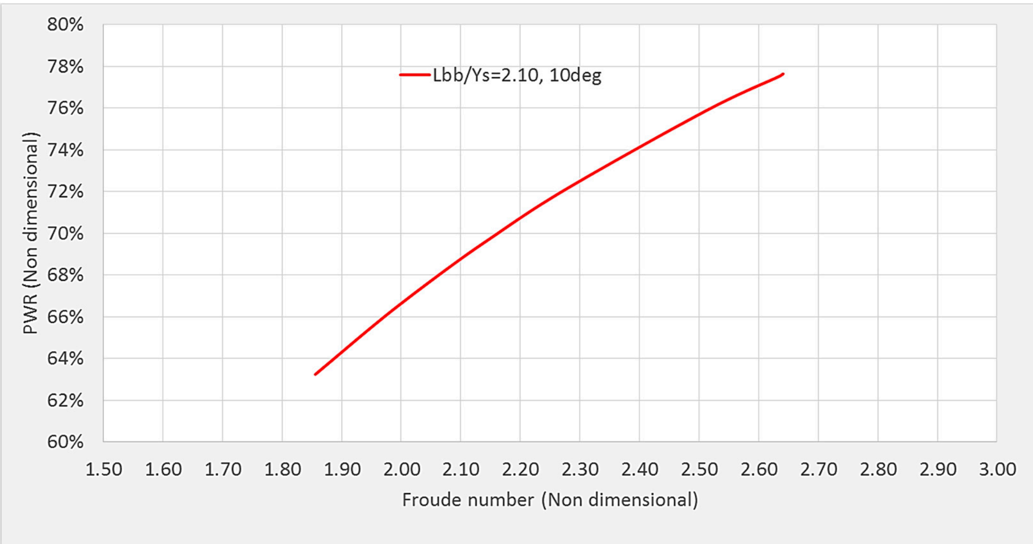

Figure 29. Proposed PWR approximation using normalized bulb length, and 10° pitch angle.

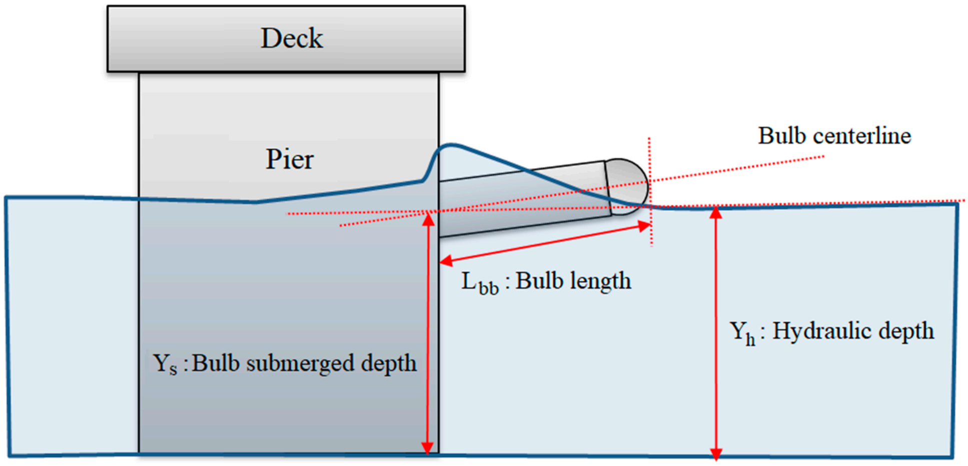

Figure 30. Definition of the bulb submerged depth and bulbous length.

5. Conclusions and Recommendations

The following are the main findings of this study:

- Experimental values show that a bulbous pier reduces the pier wave height by subtracting energy from the water flow.
- The viscous resistance is the main component in the PL_{bb}; this is due to the bulb length being less than the bulb wavelength.
- A zero-degree pitch angle bulbous pier is too long for practical applications; to achieve pier reduction in the order of 0.4, the bulb length should be above 10′.
- The introduction of the pitch angle in a bulb reduces the length of the bulb at the water line by eliminating the flow over the bulb; This modification addresses the constructability problem of a long bulbous.
- The non-bulbous pier water level (PL_{nb_calc}) overestimates the water height in comparison with the experimental data (PL_{nb_data}).
- Making the viscous resistance the only force in the calculation of B_w underestimates it.
- For practical applications, PWR_{calc} provides a good approximation to the expected reduction in the pier wave level.

Recommendations

- Full-size model trials are recommended before using a pier bulbous in lieu of pier extensions.
- A cylindrical bulbous was selected based on the literature review, but it is possible that other bulb shapes could outperform a cylindrical bulb; research is needed in this area.
- The narrow channel effect, documented in the literature review, may be responsible for the distinct bulb wave found in the 0.958′ and 0.974′; research is needed in this area.
- The pitch angles used in this research are extrapolations of the parameters used for bulbous bows on boats; determining the optimum bulb pitch angle for piers requires additional research.
- Research can be conducted on how the cantilever bulb is going to affect the structural response of the pier.

Author Contributions: Conceptualization, A.C.; methodology, A.C., M.K. and D.H.; writing—original draft preparation, M.N.-S.; writing—review and editing, M.N.-S.; supervision, M.K., D.H.

Funding: This research was funded by the Clark County Regional Flood Control District (CCRFCD).

Acknowledgments: The authors acknowledge the invaluable contribution of Mr. Peter Faught in setting up the experiments for this research.

Conflicts of Interest: The authors declare no conflict of interest.

Appendix A

Table A1. Hypothesis testing: PL_{nb} vs. PL_{bb}.

Two-Sample T-Test and CI: PLnb_T, PLbb_D, L_{bb} = 0.667′ Pitch Angle = 0°
Two-sample T for PLnb_T vs. PLbb_D N Mean StDev SE Mean PLnb_T 32000 1.323 0.239 0.0013 PLbb_D 32000 0.679 0.153 0.00085 Difference = μ (PLnb_T) − μ (PLbb_D) Estimate for difference: 0.64407 95% lower bound for difference: 0.64146 T-Test of difference = 0.7 (vs. >): T-value = −35.33 *p*-value = 1.000 DF = 63998 Both use Pooled StDev = 0.2003 *p*-value > 0.05 => DO NOT REJECT H_0 Minitab 17 report
Two-Sample T-Test and CI: PLnb_T, PLbb_D, L_{bb} = 0.958′ Pitch Angle = 0°
Two-sample T for PLnb_T vs. PLbb_D N Mean StDev SE Mean PLnb_T 32000 1.325 0.236 0.0013 PLbb_D 32000 0.636 0.142 0.00079 Difference = μ (PLnb_T) − μ (PLbb_D) Estimate for difference: 0.68873 95% lower bound for difference: 0.68619 T-Test of difference = 0.7 (vs. >): T-value = −7.31 *p*-value = 1.000 DF = 63998 Both use Pooled StDev = 0.1949 *p*-value > 0.05 => DO NOT REJECT H_0 Minitab 17 report
Two-Sample T-Test and CI: PLnb_T, PLbb_D, L_{bb} = 1.25′ Pitch Angle = 0°
Two-sample T for PLnb_T vs. PLbb_D N Mean StDev SE Mean PLnb_T 32000 1.327 0.238 0.0013 PLbb_D 32000 0.617 0.132 0.00074 Difference = μ (PLnb_T) − μ (PLbb_D) Estimate for difference: 0.71021 95% lower bound for difference: 0.70771 T-Test of difference = 0.8 (vs. >): T-value = −58.96 *p*-value = 1.000 DF = 63998 Both use Pooled StDev = 0.1926 *p*-value > 0.05 => DO NOT REJECT H_0 Minitab 17 report

Table A1. *Cont.*

Two-Sample T-Test and CI: PLnb_T, PLbb_D, L_{bb} = 1.542′ Pitch Angle = 0°
Two-sample T for PLnb_T vs. PLbb_D N Mean StDev SE Mean PLnb_T 32000 1.330 0.237 0.0013 PLbb_D 32000 0.590 0.129 0.00072 Difference = μ (PLnb_T) − μ (PLbb_D) Estimate for difference: 0.73990 95% lower bound for difference: 0.73742 T-Test of difference = 0.8 (vs. >): T-value = −39.86 *p*-value = 1.000 DF = 49433 *p*-value > 0.05 => DO NOT REJECT H_0 Minitab 17 report
Two-Sample T-Test and CI: PLnb_T, PLbb_D, L_{bb} = 1.542′ Pitch Angle = 0°
Two-sample T for PLnb_T vs. PLbb_D N Mean StDev SE Mean PLnb_T 32000 1.330 0.236 0.0013 PLbb_D 32000 0.584 0.123 0.00069 Difference = μ (PLnb_T) − μ (PLbb_D) Estimate for difference: 0.74570 95% lower bound for difference: 0.74326 T-Test of difference = 0.8 (vs. >): T-value = −36.51 *p*-value = 1.000 DF = 48 *p*-value > 0.05 => DO NOT REJECT H_0 Minitab 17 report
Two-Sample T-Test and CI: PLnb_T, PLbb_D, L_{bb} = 0.766′ Pitch Angle = 5°
Two-sample T for PLnb_T vs. PLbb_D N Mean StDev SE Mean PLnb_T 16000 1.311 0.228 0.0018 PLbb_D 16000 0.625 0.123 0.00097 Difference = μ (PLnb_T) − μ (PLbb_D) Estimate for difference: 0.68658 95% lower bound for difference: 0.68321 T-Test of difference = 0.8 (vs. >): T-value = −55.44 *p*-value = 1.000 DF = 24612 *p*-value > 0.05 => DO NOT REJECT H_0 Minitab 17 report
Two-Sample T-Test and CI: PLnb_T, PLbb_D, L_{bb} = 0.974′ Pitch Angle = 5°
Two-sample T for PLnb_T vs. PLbb_D N Mean StDev SE Mean PLnb_T 16000 1.315 0.228 0.0018 PLbb_D 16000 0.569 0.125 0.00099 Difference = μ (PLnb_T) − μ (PLbb_D) Estimate for difference: 0.74627 95% lower bound for difference: 0.74288 T-Test of difference = 0.8 (vs. >): T-Value = −26.09 *p*-value = 1.000 DF = 24860 *p*-value > 0.05 => DO NOT REJECT H_0 Minitab 17 report

Table A1. *Cont.*

Two-Sample *T*-Test and CI: PLnb_T, PLbb_D, L_{bb} = 1.266′ Pitch Angle = 5°
Two-sample T for PLnb_T vs. PLbb_D N Mean StDev SE Mean PLnb_T 16000 1.342 0.247 0.0020 PLbb_D 16000 0.4907 0.0874 0.00069 Difference = μ (PLnb_T) − μ (PLbb_D) Estimate for difference: 0.85145 95% lower bound for difference: 0.84805 T-Test of difference = 0.9 (vs. >): T-Value = −23.46 *p*-value = 1.000 DF = 19951 *p*-value > 0.05 => DO NOT REJECT H_0 Minitab 17 report
Two-Sample *T*-Test and CI: PLnb_T, PLbb_D, L_{bb} = 1.557′ Pitch Angle = 5°
Two-sample T for PLnb_T vs. PLbb_D N Mean StDev SE Mean PLnb_T 16000 1.340 0.246 0.0019 PLbb_D 16000 0.4778 0.0962 0.00076 Difference = μ (PLnb_T) − μ (PLbb_D) Estimate for difference: 0.86229 95% lower bound for difference: 0.85886 T-Test of difference = 0.9 (vs. >): T-value = −18.08 *p*-value = 1.000 DF = 20790 *p*-value > 0.05 => DO NOT REJECT H_0 Minitab 17 report
Two-Sample *T*-Test and CI: PLnb_T, PLbb_D, L_{bb} =0.787′ Pitch Angle = 10°
Two-sample T for PLnb_T vs. PLbb_D N Mean StDev SE Mean PLnb_T 16000 1.335 0.248 0.0020 PLbb_D 16000 0.571 0.112 0.00088 Difference = μ (PLnb_T) − μ (PLbb_D) Estimate for difference: 0.76362 95% lower bound for difference: 0.76008 T-Test of difference = 0.9 (vs. >): T-Value = 221263.44 *p*-value = 1.000 DF = 22258 *p*-value > 0.05 => DO NOT REJECT H_0 Minitab 17 report
Two-Sample *T*-Test and CI: PLnb_T, PLbb_D, L_{bb} =0.995′ Pitch Angle = 10°
Two-sample T for PLnb_T vs. PLbb_D N Mean StDev SE Mean PLnb_T 16000 1.334 0.249 0.0020 PLbb_D 16000 0.5207 0.0961 0.00076 Difference = μ (PLnb_T) − μ (PLbb_D) Estimate for difference: 0.81298 95% lower bound for difference: 0.80951 T-Test of difference = 0.9 (vs. >): T-Value = −41.27 *p*-value = 1.000 DF = 20666 *p*-value > 0.05 => DO NOT REJECT H_0 Minitab 17 report

Table A1. *Cont.*

Two-Sample *T*-Test and CI: PLnb_T, PLbb_D, L_{bb} = 1.286′ Pitch Angle = 10°
Two-sample T for PLnb_T vs. PLbb_D N Mean StDev SE Mean PLnb_T 16000 1.336 0.255 0.0020 PLbb_D 16000 0.5211 0.0909 0.00072 Difference = μ (PLnb_T) − μ (PLbb_D) Estimate for difference: 0.81494 95% lower bound for difference: 0.81141 T-Test of difference = 0.9 (vs. >): T-Value = −39.71 *p*-value = 1.000 DF = 19993 *p*-value > 0.05 => DO NOT REJECT H_0 Minitab 17 report
Two-Sample *T*-Test and CI: PLnb_T, PLbb_D, L_{bb} = 1.578′ Pitch Angle = 10°
Two-sample T for PLnb_T vs. PLbb_D N Mean StDev SE Mean PLnb_T 16000 1.340 0.259 0.0020 PLbb_D 16000 0.522 0.108 0.00086 Difference = μ (PLnb_T) − μ (PLbb_D) Estimate for difference: 0.81776 95% lower bound for difference: 0.81411 *T*-Test of difference = 0.9 (vs. >): T-Value = −37.08 *p*-value = 1.000 DF = 21448 *p*-value > 0.05 => DO NOT REJECT H_0 Minitab 17 report

References

1. Stonestreet, S.E.; Mulvihill, M.E.; Hite, J.E. Revised hydraulic design of the Rio Hondo Flood Control Channel. In Proceedings of the ASCE Proceeding National Conference Hydraulic, Engineering, Buffalo, NY, USA, 1–5 August 1994; pp. 401–405.
2. Hite, J.E.; Stonestreet, S.E.; Mulvihill, M.E. Model study of Rio Hondo Flood Control Channel, Los Angeles, California. In Proceedings of the ASCE Proceedings National Conference on Hydraulic Engineering, San Francisco, CA, USA, 25–30 July 1993; pp. 1695–1700.
3. Stockstill, R.L. Hydraulic Design of Channels Conveying Supercritical Flow. Available online: https://www.researchgate.net/publication/235103810_Hydraulic_Design_of_Channels_Conveying_Supercritical_Flow/related (accessed on 13 July 2019).
4. Bulbous Bow Design and Construction. Available online: http://www.mar.ist.utl.pt/mventura/Projecto-Navios-I/EN/SD-1.5.4-Bulbous%20Bow%20Design.pdf (accessed on 6 March 2018).
5. Kracht, A.M. Design of Bulbous Bows. *SNAME* **1978**, *86*, 197–217.
6. Havelock, T.H. The Wave-Making Resistance of Ships: A Study of Certain Series of Model Experiments. *Proc. R. Soc. Lon. Ser. A Contain. Papers Math. Phys. Character* **1910**, *84*, 197–208.
7. US Naval Academy: Resistance and Powering of Ships. Available online: http://www.usna.edu/NAOE/_files/documents/en400/TEXT%20%202011/12Chapter%207%20Text%202011.pdf (accessed on 6 March 2018).
8. Yun, L.; Bliault, A. *High Performance Marine Vessels*; Springer: Boston, MA, USA, 2012.
9. Ghani, M.A.; Wilson, P. Experimental Analysis of Catamarans Forms with Bulbous Operating in Shallow Waters. *Int. Shipbuild. Prog.* **2009**, *2*, 29–57.
10. Sorensen, R.M. *Basic Coastal Engineering*, 3rd ed.; Springer: Boston, MA, USA, 2006.

11. Karakouzian, M.; Karami, M.; Nazari-Sharabian, M.; Ahmad, S. Flow-Induced Stresses and Displacements in Jointed Concrete Pipes Installed by Pipe Jacking Method. *Fluids* **2019**, *4*, 34. [CrossRef]
12. Clark County Regional Flood Control District. Available online: http://www.ccrfcd.org/ (accessed on 6 March 2018).